PHILOSOPHICAL TRANSACTIONS OF THE ROYAL SOCIETY A MATHEMATICAL, PHYSICAL & ENGINEERING SCIENCES

Observing molecular dynamics with timed Coulomb explosion imaging

Ch. Ellert, H. Stapelfeldt, E. Constant, H. Sakai, J. Wright, D. M. Rayner and P. B. Corkum

Phil. Trans. R. Soc. Lond. A 1998 **356**, 329-344
doi: 10.1098/rsta.1998.0168

The Royal Society

Observing molecular dynamics with timed Coulomb explosion imaging

By Ch. Ellert[1], H. Stapelfeldt[1], E. Constant[1], H. Sakai[1], J. Wright[2], D. M. Rayner[1] and P. B. Corkum[1]

[1]*Steacie Institute for Molecular Sciences, National Research Council, Ottawa, ON, Canada K1A 0R6*

[2]*Carleton University, Departement of Chemistry, Ottawa, ON, Canada K1S 5B6*

The Coulomb explosion method for imaging molecular structure is combined with the femtosecond pump-probe technique. Thus the imaging method becomes flexible enough to determine molecular structure even in highly excited or transient states as a function of time. Examples for the applicability of this method are given. The major concerns which could limit the reliability and the accuracy of the information extracted are discussed and solutions proposed. In addition to observing time-dependent structures, optically triggered Coulomb explosion imaging can be used to identify unusual events in an ensemble of common but more frequent events.

Keywords: Coulomb explosion imaging; molecular structure; femtosecond pump-probe technique; imaging methods; pump-probe technique

1. Introduction

Coulomb explosion imaging (CEI), introduced in 1979 (Kanter 1979; Vager *et al.* 1989), is an alternative to spectroscopy for determining molecular structure. The basic principle of CEI consists of quickly ionizing a molecule thereby creating a molecular ion which dissociates quickly due to the Coulomb repulsion between the nuclei. By measuring the final velocity of the fragments one can reconstruct the initial position and thus obtain an image of the molecule. In CEI experiments performed until now, molecular ions are brought to MeV energies in large accelerators and passed through a thin foil to strip off several electrons and thereby trigger the Coulomb explosion. Alternatively, bombardment of molecules with highly charged ions has been used to remove the electrons (Werner *et al.* 1995; Mathur 1993). By means of these techniques, which employ large accelerators, ionization occurs within less than a femtosecond, as required to obtain an accurate image of the molecular wave function. The duration of high-power laser pulses is now less than 5 fs (Nisoli *et al.* 1997) so they are only one order of magnitude longer than the typical transit time of a MeV molecule through a foil. Thus, at least for heavy molecules, femtosecond pulses can replace accelerators as a means of initiating Coulomb explosions, since the electrons can be stripped fast enough from the molecule before the heavy particles start moving.

Viewed from the perspective of the 1990s, spectroscopists have determined the equilibrium structure of most small molecules and so there is little motivation for reproducing the successes of spectroscopy. What makes optically triggered Coulomb

explosion imaging especially exciting from the current perspective is the fact that the combination of femtosecond pump-probe technology with the capabilities of Coulomb explosion technology allows imaging of excited states and photochemical dynamics (and, as we shall see, other reactions).

Timed CEI offers two advantages over the currently developed X-ray (Raksi *et al.* 1996) and electron diffraction (Williamson *et al.* 1997) methods for following time-dependent structural changes during photochemical processes. First, the time resolution with femtosecond lasers can be brought to 5 fs, while the shortest X-ray pulses achieved so far with $\lambda \leqslant 1$ Å have a duration of 300 fs (Schoenlein *et al.* 1997) and the electron bursts are as long as 20 ps (Williamson *et al.* 1997). Second, by observing the fragments coming from the exploding molecule and integrating the velocity vectors backwards in time one obtains the molecular structure directly from one explosion event. In contrast, in the diffraction experiments one needs to collect a large amount of scattering data from which the structural information has to be extracted by Fourier transform.

What distinguishes optically driven Coulomb explosion from traditional pump-probe dynamics experiments? Since the Fourier transform relates the time and frequency domain, weak field pump-probe experiments are unlikely to give us revolutionary insight not available from frequency-dependent experiments, although time-dependent experiments may be much easier to analyse than frequency domain experiments in many cases. In contrast, timed CEI has no frequency domain analogue, since the strong field cannot be considered as a weak perturbation.

The three aims of this paper are dealt with in separate sections. In § 2, two experiments on diatomics are described in which the capability of CEI to measure the space and time evolution of a molecular wavepacket $|\Psi(\boldsymbol{r},t)|^2$, is demonstrated. In § 3, the physical concepts and the conditions, under which the experiments have to be performed and how they can be fulfilled are discussed. In using CEI one has to be concerned about the movement of the atoms during the ionizing laser pulse, the deviation of the internuclear potential from the perfect Coulombic behaviour, the dependence of the ionization probability on the laser polarization and the internuclear distance, and the influence of the laser field itself on the ions, i.e. the deformation of the molecular potential surfaces by the strong laser field. The latter three of these four major concerns are dealt with in more detail in the corresponding subsections. Finally, two general approaches are discussed in § 4 for exploiting the advantages of the short pulse laser induced CEI.

2. Coulomb explosion of I_2

Two examples are given here to demonstrate the measurement of the molecular wave function, $|\Psi(\boldsymbol{r},t)|^2$ (Stapelfeldt *et al.* 1995), by the time-dependent Coulomb explosion imaging technique. First, a dissociating wavepacket in I_2, second an exotic wavepacket formed by a doubly peaked optical pulse (Stapelfeldt *et al.* 1997*a*), were imaged by Coulomb explosion. The dissociating I_2 molecule was chosen to illustrate the potential of timed Coulomb explosion imaging. After initiating the photodissociation with a femtosecond pump pulse (see figure 1), the position measurement was performed by initiating the Coulomb explosion with a delayed probe pulse and by subsequently determining the kinetic energy of the exploded fragment ions in a time–of–flight (TOF) mass spectrometer.

Since the experiments have been described in detail (Stapelfeldt *et al.* 1995, 1997*a*),

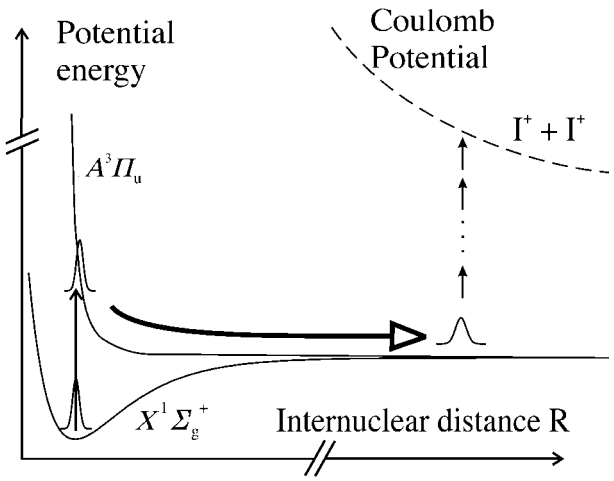

Figure 1. Schematic of the relevant potential energy curves of I_2 illustrating the formation of a moving wave packet in the dissociative state and its subsequent projection onto a repulsive Coulomb potential curve.

only a short description is given here. Iodine molecules were expanded with helium through a nozzle into a vacuum chamber maintained at a pressure of less than 10^{-8} mbar. The laser beam intersected the molecular beam at 90°. The ions were extracted into the TOF spectrometer at 90° with a typical voltage $U_{\mathrm{TOF}} = 600$ V. This acceleration and the subsequent field-free drift region were of equal length, $L = 3$ cm. Finally, the ions were post-accelerated by 2 kV and detected by a dual micro channelplate. Apertures restricted the angular acceptance of the TOF so that only molecules exploding with fragments directed along the flight axis could be observed.

The 80 fs, 625 nm pulses were generated by an amplified colliding pulse mode-locked (CPM) dye laser and separated into a weak pump and an intense probe pulse by a beam splitter. The pump pulse (peak intensity about 10^{12} W cm^{-2}) excited the molecule to a dissociating state (figure 1), here $A^3\Pi_u$. The intense probe pulse, arriving at a specified time delay, ionized the molecule to produce I_2^{n+}.

The velocity, v, that the fragments obtained due to the Coulomb repulsion was measured by the deviation of their flight time from that expected for a zero velocity fragment with the same mass to charge ratio, m/q. Those exploding towards the detector arrived earlier than those ejected away from the detector. The time separation between the early and late arriving fragments is $\Delta t = 2vmL/(qU_{\mathrm{TOF}})$. Assuming only Coulomb repulsion is responsible for the observed velocity distribution, Coulomb's law allows us to reconstruct the distribution of internuclear distances $\boldsymbol{r}$ at the time t of the measurement, i.e. $|\Psi(\boldsymbol{r},t)|^2$. In fact, it can be shown that even though the ionic cores have an initial velocity caused by the single photon dissociation step, $|\Psi(\boldsymbol{r},t)|^2$ can be deconvoluted from the measured time of flight distribution (Stapelfeldt *et al.* 1997*b*). Figure 2 shows images of $|\Psi(\boldsymbol{r},t)|^2$, taken at different time delays between the pump and probe pulses. The spatial resolution is 2 Å in the region of internuclear separations from 5 to 15 Å combined with a time resolution of 80 fs, given by the duration of our probe pulse.

As a second example we demonstrate that even complex unusual wavefunctions—here: a double-peaked wave function evolving in the $A^3\Pi_u$ state—can be measured by CEI. By adding a birefringent quartz plate along the optical path of the pump beam

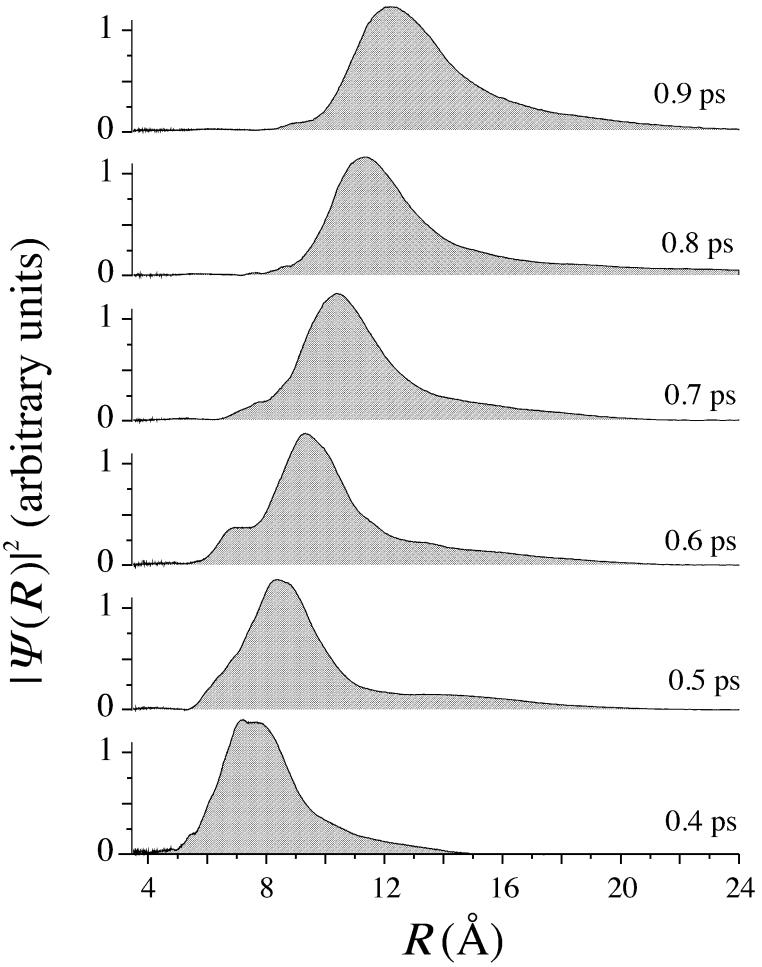

Figure 2. The square of the internuclear wavefunction, $|\Psi(\boldsymbol{r},t)|^2$, of the dissociating I_2 molecule measured at different times after excitation by a single pump pulse. Each trace is an average of 2000 shots.

two successive pump pulses can be produced (Stapelfeldt *et al.* 1997*a*). Their time separation is determined by the difference of optical thickness of the quartz plate along its two axes. Their relative energy is determined by the angle between the optical axis and the laser polarization. Following the same procedure outlined above we can measure $|\Psi(\boldsymbol{r},t)|^2$. The double-peaked wave packet (figure 3) represents a 'Schrödinger cat-like' state since each molecule experiences a double-peaked optical pulse each of which promotes only a fraction of the ground-state population into the excited state.

3. Fundamental considerations of CEI

The above-described experiments illustrate the potential of timed Coulomb explosion imaging. However, in order to apply this method to more complex chemical processes four major concerns connected with CEI need to be addressed. Since they

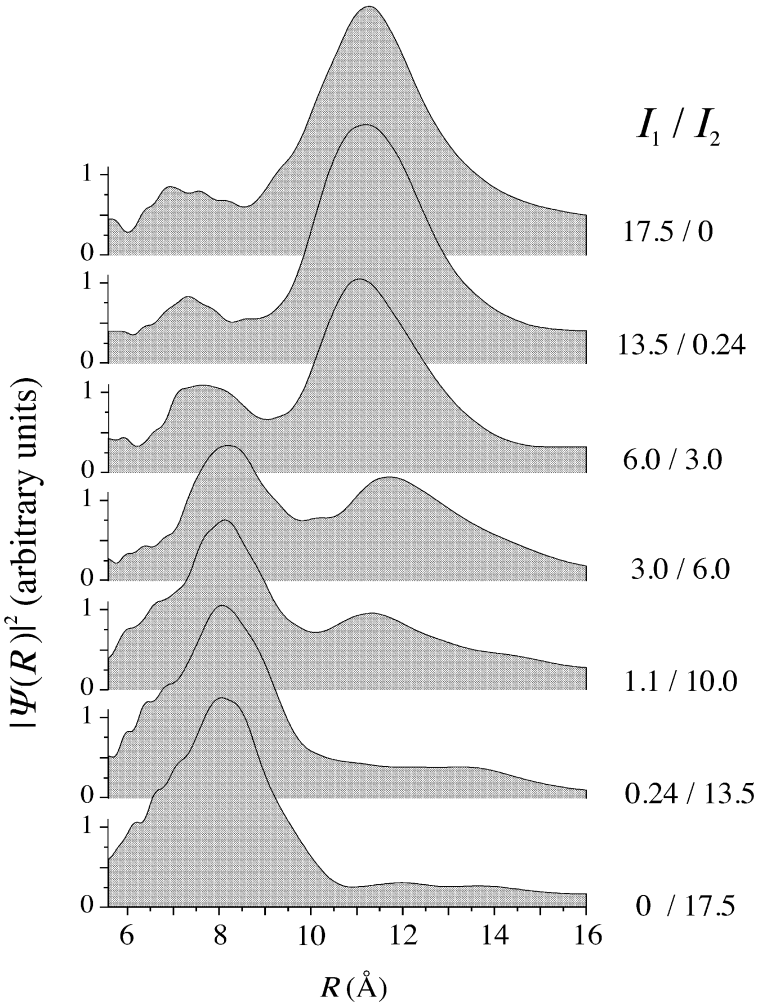

Figure 3. The square of the internuclear wave function, $|\Psi(\boldsymbol{r},t)|^2$, when two pump pulses are used to dissociate iodine. The different traces correspond to different intensity ratios of the two pump pulses (units for the intensity are 10^{12} W cm^{-2}). Each trace is an average of 2000 laser shots and is recorded 810 and 500 fs after exposure to the first and second pump pulse, respectively.

can be overcome only partly by using sufficiently short laser pulses they need to be discussed in more detail in the following subsections.

(i) The ionizing pulse must be short enough to freeze even highly charged molecular ions by their own inertia for the duration of the ionizing pulse. In our iodine experiments the 2 Å resolution is mainly determined by the internuclear motion within the 80 fs pulse. With high power 5 fs pulses (Nisoli *et al.* 1997), ion motion during ionization is a limitation only for low-mass ions (less than 20 amu).

(ii) The field-free potential structure of the molecular ion should not deviate too much from the Coulombic behaviour, since Coulomb's law is used to convert from the measured kinetic energy to internuclear positions (see § 3 *a*).

(iii) It has been shown theoretically and experimentally that the ionization rate is extremely sensitive to the internuclear separation, R, for a molecule with the inter-

nuclear axis aligned to the laser polarization but almost independent of R when the molecular axis is perpendicular to the field (see § 3 *b*, *c*). The sensitivity of the ionization rate to internuclear separation would lead to an error in measurement of $|\Psi(\boldsymbol{r},t)|^2$, which was avoided in the I_2 experiment described above by using perpendicularly polarized light and large internuclear distances. Furthermore, this sensitivity to internuclear separation and orientation requires that in experiments with polyatomic molecules only one exploding molecule will be imaged at a time. Thus the orientation of the molecule with respect to the laser polarization can individually be taken into account.

(iv) The interaction between the laser field itself and the molecule must not perturb the measurement process (Dietrich *et al.* 1993), i.e. the ions should not be accelerated by the electric field of the laser itself but only by the Coulomb repulsion. In other words the electronic potential of the exploding molecular ion should not deviate significantly from the field-free potential. For 5 fs pulses, the ion motion while the molecule is in the strong laser field will be a concern only for low-mass ions. For these ions, an acceleration in the direction of the internuclear axis changes the observed explosion velocity of the fragments and thus influences the inferred position of the fragment at the instance of the ionization; an acceleration perpendicular to the internuclear axis influences the detection efficiency of the fragments. The latter effect is commonly referred to as strong-field alignment and will be discussed for diatomic molecules in § 3 *d*.

(*a*) *Deviations from Coulomb potential in highly charged I_2 ions*

Critical to the concept of Coulomb explosion imaging, no matter if the explosion is driven optically or by rapid passage through a foil, is the validity of Coulomb's law to describe the internuclear force between ions. Molecular bonding will cause deviations for many molecules and the order-of-magnitude of these forces must be estimated. Studies of the halogen ions are particularly interesting for these estimates since the outer electrons are in anti-bonding orbitals and removing them increases the bond order, i.e. the excess of bonding over antibonding electrons. Consequently, the deviation from Coulomb's law will be larger than in most other molecular ions.

Calculations of the potential curves for the iodine diatomic ions I_2^{n+} (Corkum *et al.* 1997) with $n = +2$ to $+6$ were performed using *ab initio* calculations which included averaged relativistic effective core potentials (Hurley *et al.* 1986) with corrections for spin-orbit coupling. An spd valence basis set included three each of s, p and d-type functions. The SCF MOs were generated for the closed-shell iodine molecule and were used for all the ionic states. A configuration selection scheme based on energy lowering resulted in inclusion of about 40 000 spin-orbit states in the final calculation.

In figure 4 we show the deviation from a purely Coulombic interaction for the various molecular ions. All curves become Coulombic for $R > 5$ Å. Therefore, the measurement of $|\Psi(\boldsymbol{r},t)|^2$, in figures 2 and 3 for $R > 5$ Å is not affected by the deviation from Coulombic behaviour.

The trends in figure 4 can be discussed with reference to molecular bond order. The total bond order is 1.0 in the ground state of I_2 molecules leading to a small well depth of 1.56 eV. In the case of I_2^{2+} the bond order has increased to 2.0 due to the loss of two antibonding electrons and the deviation from Coulomb's law has a maximum value of 1.7 eV. As the next two electrons are lost we form I_2^{3+} and then I_2^{4+} and the bond order is increased to 2.5 and then 3.0. The deviation from Coulomb's law continues to increase. The trication, I_2^{3+}, (and the other halogen ions

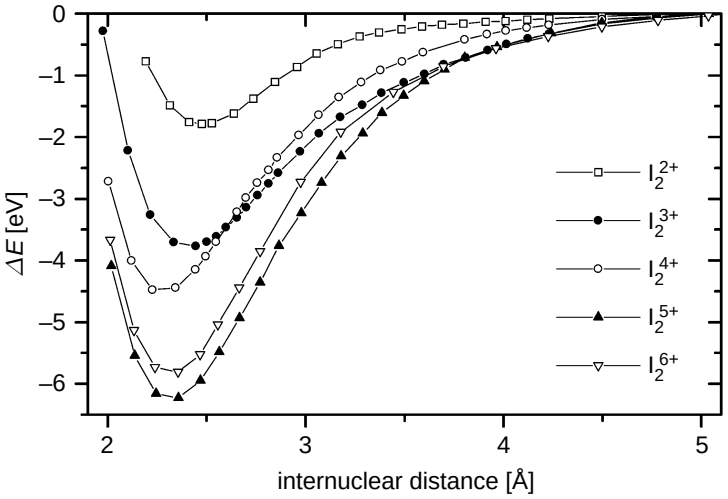

Figure 4. Deviation of the quantumchemical internuclear potential from the Coulombic behaviour in I_2^{n+} for $n = 2, \ldots, 6$.

Cl_2^{3+} and Br_2^{3+}) even has a metastable ground state as is shown in figure 5 where we plot the portion of the TOF spectrum corresponding to the arrival time of these molecular ions. The reader is referred to Harbol (1995) and Sakai *et al.* (1997) for a full discussion of these species. The calculated lifetime of Cl_2^{3+} exceeds 1000 years (Sakai *et al.* 1997). Only when we reach I_2^{4+} do we observe a fully repulsive potential curve. If we assume Coulomb's law governs the internuclear reaction rather than the potential curve shown in figure 4 we will make a maximum error of about 0.5 Å in an inversion procedure with the error decreasing rapidly with increasing charge of the molecule.

(*b*) *The strong dependence of the ionization rate on the internuclear coordinate*

Coulomb explosion imaging is effective with three very different ionization mechanisms; electron stripping by rapid passage through a thin gold foil, by highly charged ion passage or by femtosecond strong-field ionization. Therefore, it is clear that details of the ionization mechanism are not of critical importance for the imaging of the structure from the measured fragment velocities, provided that the stripping process is fast enough. In this section we show what characteristics are unique in strong-field ionization, the understanding and exploiting of which will open new applications for Coulomb explosion imaging (see § 4).

Already we have used our knowledge of the unique characteristics of strong field ionization in the described experiment, because an accurate determination of the time-dependent wave packet structure requires a knowledge of the ionization rate as a function of the internuclear separation (figures 2 and 3). The tacit assumption in § 2, that the ionization rate was independent of the internuclear separation R, is approximately true in a strong field only for molecular ions oriented with internuclear axis perpendicular to the laser electric field. Therefore, the exploding laser polarization was chosen perpendicular to the internuclear axis in the described wave packet experiments.

However, for molecular ions with the internuclear separation parallel to the laser electric field there is a so-called enhanced ionization region located at approximately 1.5–2 times the equilibrium internuclear distance of the neutral molecule. In this

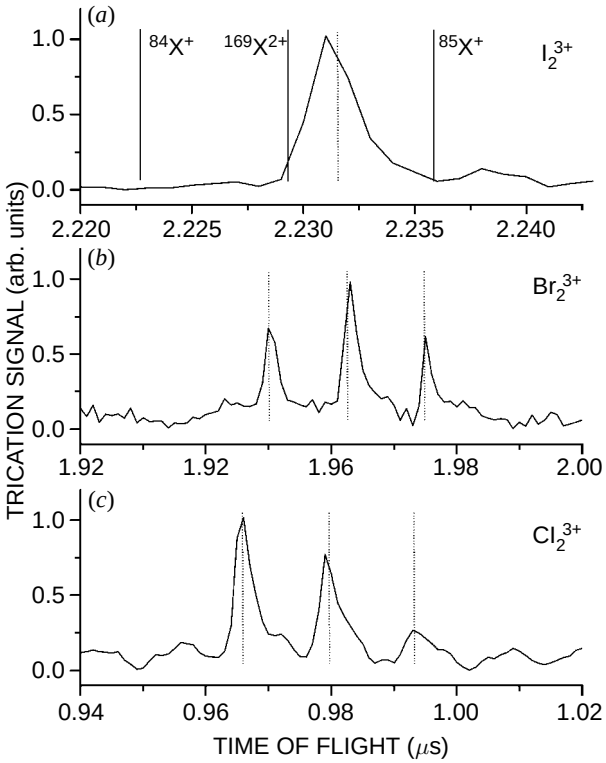

Figure 5. TOF spectrum showing the region around the arrival time of the metastable iodine, the bromine and the chlorine triply charged ions. The dotted lines show the anticipated positions of the trications calibrated with well-known species. The positions of the singly charged mass 84 and 85 peaks and the positions of the doubly charged mass 169 are included in (*a*) for reference.

region the ionization rate is predicted to reach a maximum that is many orders of magnitude greater than the ionization rate at smaller or larger internuclear separations (Chelkowsky & Bandrauk 1995; Seideman *et al.* 1995).

One way to explain this enhanced ionization effect is as follows. Figure 6 shows the structure of the Coulomb potential as seen by a single electron moving in the potential of two ions modified by the strong laser field. Two views of the molecule are shown. The first one is the front view in which the ions are side–by–side and the electron moves in a double well potential structure, which has to be considered when the field is polarized along the internuclear axis. In this case the electron motion along the field is influenced by the two wells. The end view shows the potential structure the electron experiences in the plane perpendicular to the molecular axis; in that case one well only influences the electron motion.

A molecule viewed from the end looks much like an atom. It would not be surprising if we could use atomic ionization theories to describe molecular ionization in this case. In fact, this is possible (Chin *et al.* 1992). Molecules, when viewed from the front are very different from atoms. It is impossible that tunnel ionization to the continuum would not be severely affected by these two different projections of the molecule, as explained in the following paragraph.

Figure 7 shows the side view potentials of a diatomic molecule at three different internuclear separations. For small internuclear separation (dotted line) the electron can move freely between the two nuclei following the laser field. At an intermedi-

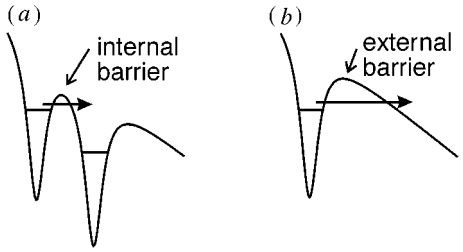

Figure 6. Schematic structures of the Coulomb potential with superimposed laser electric field as seen by a single electron moving in the potential of two ions. The side view shows the ions side–by–side, the electron moves in a double well potential structure, relevant for laser polarization along the internuclear axis. The end view shows the potential structure the electron experiences in the perpendicular plane, which is relevant for laser polarization perpendicular to the internuclear axis.

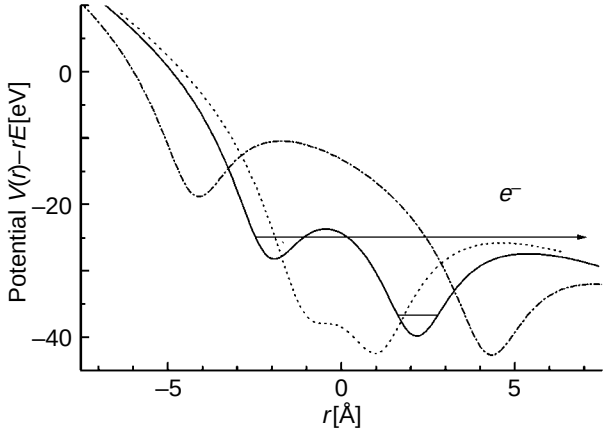

Figure 7. Potential seen by an electron in the presence of a DC electric field parallel to the molecular axis, for three values of internuclear separation. The arrow shows the new ionization channel due to tunnelling through the internal barrier directly to the continuum.

ate internuclear separation (solid line) the electron has a significant chance of being trapped in the up-hill well as the laser field changes sign. The dash-dotted line illustrates the case of large internuclear separation. It is clear from the three curves that the tunnelling rate will be much greater (the tunnelling rate depends exponentially on the product of the barrier height and width) for the electron trapped in the upper well at the characteristic internuclear separation at which this occurs than for either smaller or larger separations (Codling *et al.* 1989).

There is a second way (Seideman *et al.* 1995) to see that the ionization rate of a diatomic molecule oriented parallel to the laser field must vary strongly with the internuclear separation. At large internuclear separation the tunnelling rate of a molecular ion should be approximately calculated from the tunnelling rate of the lowest charged atomic or ionic constituents in the combined fields of the laser and the adjacent ion. Since tunnelling is a nonlinear function of the field, the combined fields of the laser and the adjacent ion must augment the tunnelling rate over the rate without the ion present. Ionic fields can be very strong and so the augmentation in the tunnelling rate can be very large as the internuclear separation becomes small. The field produced by a single charge at a distance of 2.5 Å (corresponding to the peak of the barrier for an internuclear separation of about 5 Å) is 2.3×10^8 V cm^{-1}.

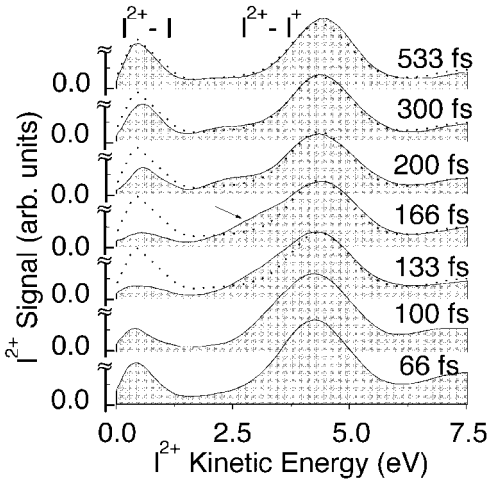

Figure 8. Demonstration of the enhanced ionization for parallel polarization. The I^{2+}–I signal around 166 fs is significantly suppressed.

The same peak field is reached in a pulse of approximately 10^{14} W cm^{-2} peak laser intensity.

The rate cannot increase without limit because we also know another limit. When the internuclear separation is shrunk to zero, H_2^+ becomes He^+ (neglecting the neutrons), which has a very high ionization potential and a correspondingly low ionization rate. The rate must peak at some internuclear separation and this separation is likely to be near the region in which the charge localizes on one ion or the other and is therefore unable to jump from one atom to the other atom as the field changes.

(*c*) *Experimental test of enhanced ionization*

To experimentally control the internuclear separation of a molecule and therefore measure the ionization rate as a function of its internuclear separation we employ a molecular wavepacket (Constant *et al.* 1996). That is, instead of focusing our attention on strong fields as a diagnostic of femtosecond molecular dynamics (discussed in § 2 in connection with Coulomb explosions) we use femtosecond dynamics to diagnose strong-field processes. This basic approach should be useful for studying the potential curves of highly charged molecular ions as well.

The experiment was performed (Constant *et al.* 1996) using the same experimental arrangement that was used for the Coulomb explosion experiment (discussed in § 2) except the pump pulse was intense enough to produce I_2^{2+}. We concentrated on the dissociation channel leading to $I^{2+}+I$. In that channel the pump pulse produces a dissociative wave-packet moving with an asymptotic velocity of 20.6 Å ps^{-1}. Figure 8 shows the probability of observing the $I^{2+}+I$ channel after exposure to both the pump and the probe pulse as a function of the delay between the pulses (the weaker probe pulse is polarized parallel to the internuclear axis). The depletion of the $I^{2+}+I$ channel is centred around 166 fs and indicates the existence of an enhanced ionization region. The delay of 166 fs corresponds to an internuclear distance of about 6 Å in good agreement with the predictions of the enhanced ionization model (Seideman *et al.* 1995). No enhanced ionization is observed when the probe pulse is polarized perpendicular to the molecular axis.

(*d*) *Alignment during dissociative ionization*

To obtain an accurate image by CEI it is essential that the arrangement of the nuclei in an exploding molecule is not affected by the high-intensity pulse that triggers the explosion. This is a concern since an intense laser field always induces instantaneously a dipole moment in a molecule which in turn interacts with the laser field and thus gives rise to a torque on the parent molecule (Dietrich *et al.* 1993) or on a molecular subunit. This torque leads to an angular momentum of the molecule or a subunit and, if strong enough, can reorient it, distorting the image to be taken by measuring the momenta of the fragments. The image-distorting effect of the reorientation of the molecule as a whole can in principle be circumvented by taking the image of a single molecule at a time by means of a position- and time-sensitive detector. However, the image distortion due to reorientation of a subunit (in the case where a polyatomic molecule dissociates quickly during the laser pulse) is more severe and needs a quantitative understanding of the forces involved in the reorientation effect.

To this extent, we started to investigate the role of the molecular mass on the alignment effect during strong-field dissociative ionization in a series of diatomic molecules. Qualitatively, the alignment can be understood as follows. During the laser pulse, as the atomic cores separate, the torque increases until the nuclei are far enough apart that the electrons localize on one of them, thus reducing the polarizability to the atomic value. Localization of the electron (bond cleavage) occurs at an internuclear separation of about 1.5–2 times the equilibrium distance.

It has been proposed (Normand *et al.* 1992; Strickland *et al.* 1992; Codling *et al.* 1993) that the molecular reorientation becomes evident in dissociative ionization experiments in which the kinetic energy spectra for various polarizations are compared. The mass of the constituent atoms has to be carefully considered. Qualitatively, lighter molecules (O_2, Cl_2) with a smaller moment of inertia (compared to iodine) orient faster for a given torque. Thus, molecules from a larger angle of acceptance can reach the detector, giving rise to a higher signal. On the other hand, the lighter atoms move apart faster as soon as they reach a higher charge state. This increases the moment of inertia and decreases the angular velocity. Furthermore, the time during which the torque is acting on the molecule is reduced.

In fact, it is now widely assumed that during all strong-field dissociative ionization experiments for all masses to date, strong molecular reorientation occurs. These experiments are cited as evidence of the ability of strong fields to align and orientationally trap neutral molecules (Friedrich & Herschbach 1995) and to justify the use of linear models for strong-field theories (Brewczyk *et al.* 1997). If these dissociative ionization experiments are correctly interpreted, it is essential to consider how short the intense laser pulse must be before these effects can be neglected in the Coulomb explosion image.

However, observing angle-dependent fragmentation does not clearly imply molecular reorientation. Dissociative ionization is explained as follows:

(i) the molecules reach a dissociative state;

(ii) the molecule reorients along the laser polarization both before and during the dissociation;

(iii) inization continues (with enhanced probability) as the molecule dissociates.

The final process, that the molecule enters a region of enhanced ionization as it dissociates, has already been discussed in §§ 3*b* and 3*c*, where it was also shown that enhanced ionization is strongly dependent on the molecular orientation. Thus,

even without molecular re-alignment, charged fragments are much more likely to be produced from molecules aligned parallel to the field than perpendicular. This angular dependence of enhanced ionization is so strong that it can mask molecular reorientation in many diatomic dissociative ionization experiments.

To disentangle reorientation and enhanced ionization during dissociative ionization, we introduce a new measurement scheme in which we compare the kinetic energy distribution for linear laser polarization parallel to the detector axis (because of the apertures in our TOF mass spectrometer we observe only molecules that explode along this axis) with the kinetic-energy distribution for circular polarization with the same maximum electric field. The intensity of the cicularly polarized laser beam is therefore twice the intensity of the linearly polarized beam. The basis of the technique is that the enhanced ionization efficiency for circularly and parallel polarized light is identical provided that their electric field vectors parallel to the molecular axis are the same. This equality of the electric field component parallel to the detector axis is achieved by using a first-order quarter waveplate and a polarizer. Circularly polarized light is obtained by placing first the polarizer in the initially linearly polarized laser beam (the polarizer is parallel to the incoming polarization and to the TOF axis) followed by the $\frac{1}{4}\lambda$ plate at an angle of 45°. By interchanging waveplate and polarizer but keeping their respective angle fixed, the laser beam, after the two components, is again linearly polarized but has excactly half the intensity of the circularly polarized light and the same electric field component parallel to the polarizer axis. Perpendicular or parallel polarization with respect to the detector axis is then simply obtained by rotating the polarizer. Since the number of surface reflections is equal to the remaining difference in electric field component between circularly and linearly polarized light is due to imperfect matching of the wave plate to the used laser wave length. The difference in parallel field component was measured to be better than 3%.

The hypothesis of approximately equal ionization rate for circular and parallel polarization with equal electric field component along the molecular axis is verified in a separate experiment on CH_2I_2, where the alignment effect (process (ii)) can be excluded due to the large momentum of inertia of this molecule and the large separation of the iodine atoms. Note, that the iodine atoms have a ground state internuclear separation of 3.5 Å (Baughcum & Leone 1980)† which corresponds approximately to the distance at which the ionization rate of I_2^{n+} is maximum‡. We assume that this 'quasi-diatomic' iodine is nearly unaffected by the carbon and hydrogen atoms since—due to their low mass—they quickly leave the surroundings of the I_2. Thus, this molecule can be used as a test case where an iodine molecule is formed at a large internuclear separation while any alignment is entirely absent. From figure 9 it is clear that the ionization efficiency is nearly identical for parallel and circularly polarized light with equal maximum field.

In order to establish the comparison of kinetic energy distributions for linearly and circularly polarized light as a valid method to exclude alignment effects in the dissociative ionization one has to be concerned if the probability that the molecule reaches the dissociative state (i.e. process (i)) is the same for linearly and circularly

† A quantum mechanical calculation with a modern commercial code gave a bond length of 3.86 Å (R. Yip, personal communication).

‡ The critical distance is approximately twice the equilibrium distance in the ground state (M. Yu Ivanov, personal communication).

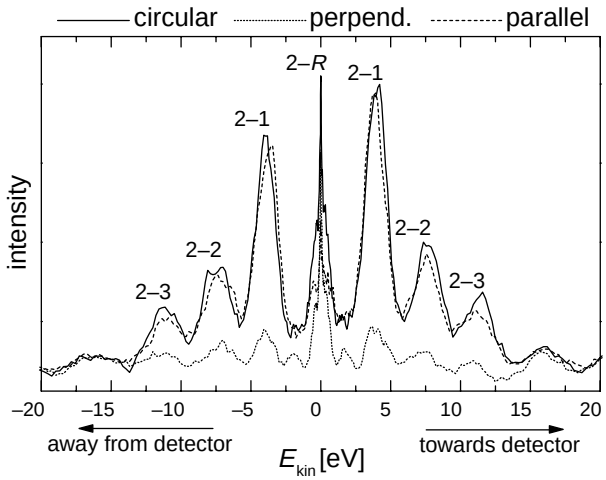

Figure 9. Distribution of the kinetic energy of I^{2+} after dissociative ionization of CH_2I_2 for circular and linear laser polarization, parallel and perpendicular to the detector axis. The kinetic energy is plotted positive for ions ejected towards the detector and negative for ions ejected away from the detector. The alignment of this molecule can be excluded due to the arguments given in the text. The central peak 2–R is due to the dissociation of the doubly charged parent molecule into I^{2+} and a radical. The peaks attributed to Coulomb explosion channels I^{2+}–I^{n+} are labelled 2–n. The intensity distribution is nearly identical for both circular and parallel polarization, indicating that the ionization of the molecule is dominated by the magnitude of the electric field vector parallel to the molecular axis. The small peaks at the edges of the pattern are due to ringing in the detector and cover the I^{2+}–I^{4+} peaks.

polarized light. Experimentally, we have some evidence that the behaviour for both polarizations is similar. The kinetic energy spectra (figure 9) of the lowest energy fragments, which come from the focal region of relatively low laser intensity, show a linearity in the electric-field components. The intensity distribution for the circular polarization is nearly the sum of the parallel and perpendicular polarizations. Thus, the laser field components parallel and perpendicular to the molecular axis can be treated separately. The width of the central peak tells us about the kinetic-energy release from the low charge state I_2^{2+}. This release is equal for linear and circular light. Therefore, we assume that, for low laser intensities on the time scale of 80 fs, the equivalence of parallel and circular light with equal parallel electric-field component is well founded.

Having established the assumption that parallel and cicular laser polarization with identical electric-field vector parallel to the molecular axis have the same ionization efficiencies, we can introduce the measurement scheme for studying quantitatively the alignment effect as a function of molecular mass. For circular polarization the torque acting on the molecule during one laser cycle averages to zero since during one half of the optical cycle the torque turns the molecule towards the detector axis and during the other half cycle towards the axis perpendicular to the detector. Therefore, for parallel laser polarization the number of molecules which are exploding along the detector axis should increase compared to circularly polarized light if alignment plays a significant role.

In figure 10 the fragmentation pattern obtained by detecting the doubly charged atomic ions are compared for O_2, Cl_2 and I_2, in the cases of parallel, perpendicular and circular laser polarization. For iodine the magnitude of the signal is the same for circular and parallel polarization while for Cl_2 and O_2 the ionic signal is clearly

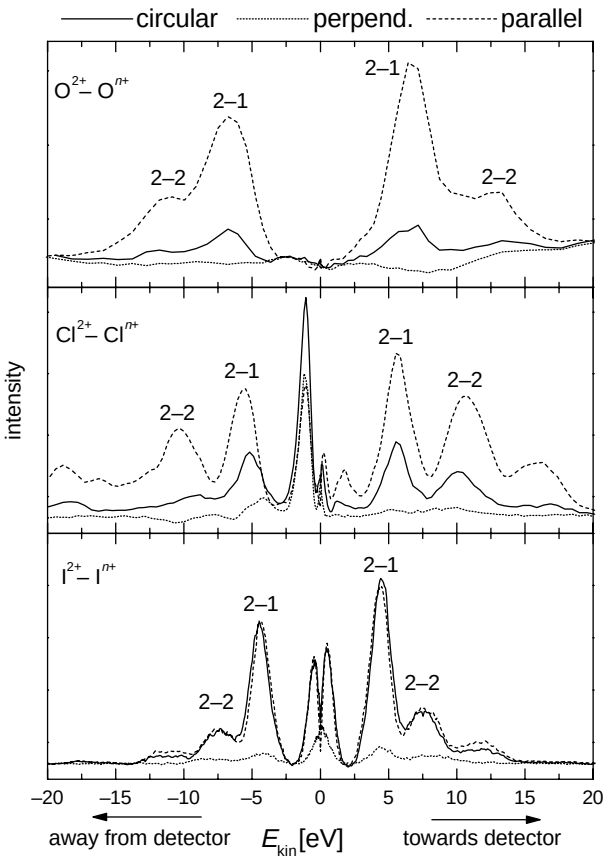

Figure 10. Comparison of the explosion pattern of O_2, Cl_2 and I_2. The kinetic energy distribution of the doubly charged fragments is compared for circular and linear polarization, either perpendicular or parallel to the TOF axis. For parallel and circular polarization the detected intensity distribution is equal for the heavy iodine, while for lighter molecules the parallel polarization produces a strongly enhanced signal. The electrical field vector was kept constant for all three polarizations. Due to the smaller acceptance angle of the detector for the backwards ejected ions, their intensity is lower compared to the ionic fragments of equal kinetic energy ejected towards the detector. The strong peak in the Cl_2 pattern near 1 eV backwards is due to H_2O^+ contamination.

stronger for parallel than for circular polarization. Therefore, for oxygen and for chlorine many more molecules are reoriented along the laser polarization while for iodine reorientation plays no role in the regions of the focal spot where the laser intensity exceeds the threshold intensity for fourfold charged molecules.

It becomes clear from figure 10 that I_2 does not align with the laser polarization ($I_{\mathrm{peak}} = 10^{15}$ W cm^{-2}, FWHM = 80 fs). However, the laser pulse polarized parallel to the molecular axis allows the production of I_2^{5+} (the 2–3 channel appears in figure 10) while the pulse of the same intensity but polarized perpendicularly to the molecular axis allows only the production of triply charged ions (maximal the 2–1 channel in the perpendicular trace in figure 10). This difference in magnitude of the ionic signal for perpendicular and parallel polarization can now fully be attributed to the enhanced ionization effect (see § 3 *c*).

Our results indicate that molecular re-alignment is present in dissociative ionization experiments and will influence CEI if the length of the laser pulse is significant

on the time scale of molecular vibration or rotation. However, in such cases as I_2 where the pulse duration is shorter than the characteristic time for dissociation, re-alignment is a small effect. Only in the case of much lower masses does re-alignment contribute significantly to the anisotropic detection efficiency.

4. Conclusion

Two general categories of applications of CEI can be foreseen: (i) observation of the evolution of time-dependent processes (taking a femtosecond movie frame–by–frame with a temporal resolution limited by the duration of the pulse and not by its spectrum); and (ii) selection of unusual events of interest from a large ensemble of frequent but common events. The former falls within the normal direction of femtosecond science, the latter is new and makes use of the particle-physics-like nature of Coulomb explosion imaging. In conclusion we briefly discuss each.

(i) *Time-dependent photochemical processes*.

(a) For small polyatomic molecules it should be possible to obtain time-dependent images of the detailed atomic positions during a photochemical process by measuring the velocities of all fragment ions of the Coulomb explosion. The iodine experiments described in § 2 are precursors to these kinds of experiments.

(b) For larger molecules it is unlikely that the detailed positions of all atoms are of interest, but instead the more general structure. It should be possible to obtain information about the time dependence of coarse structural changes during a photochemical process of larger polyatomic molecules by measuring the velocities of particular ionic fragments only. These could be either larger subgroups, geometrically exposed constituents or selected atoms in the molecule (such as nitrogen, iodine or other atoms). From the velocities of these selected fragments only, we should be able to reconstruct the general features of the photochemical process.

(ii) *Selecting unusual events of interest from a large ensemble*.

(a) Perhaps the most exciting prospect is to identify specific important structures that a molecule experiences. One important unusual (transient) structure is the transition state of a polyatomic molecule. Since the internuclear separation in the transition state is in the critical region where the ionization rate is enhanced, ionization of a molecule in this state is favourable. Thus enhanced ionization forms a basis for selection of this particular configuration for analysis.

(b) It should also be possible to identify characteristic structures during binary collisions in beam (or gas cell) experiments by Coulomb exploding the colliding partners. The characteristic of a collision is a significant change in kinetic energy of either product or fragment. The existence of these energetic fragments allows us to rapidly select the interesting events (atoms in close collisional contact with a molecule) from the large number of common events (atoms that are distant from molecules).

Each of these experiments represents a new direction in femtosecond science.

The authors acknowledge discussions with M. Ivanov, T. Seideman, A. Stolow, the potential energy curve calculations by G. DiLabio and the valuable technical assistance of D. Joines. Ch.E. benefits from the financial support of the Alexander von Humboldt Stiftung.

References

Baughcum, S. L. & Leone, S. R. 1980 Photofragmentation infrared emission studies of vibrationally excited radicals CH_3 and CH_2I. *J. Chem. Phys.* **72**, 6531.

Brewczyk, M., Rzazewski, K., Clark, C. W. 1997 Multielectron dissociative ionization of molecules by intense laser radiation. *Phys. Rev. Lett.* **78**, 191.

Chelkowsky, S. & Bandrauk, A. D. 1995 Two-step Coulomb explosions of diatoms in intense laser fields. *J. Phys.* B **28**, L723.

Chin, S. L., Liang, Y., Decker, J. E., Ilkov, F. A. & Ammosov, M. V. 1992 Tunnel ionization of diatomic molecules by an intense CO_2 laser. *J. Phys.* B **25**, L249.

Codling, K., Frasinski, J. & Heatherly, P. A. 1989 On the field ionisation of diatomic molecules by intense laser fields. *J. Phys.* B **22**, L321.

Codling, K. & Frasinski, J. 1993 Dissociative ionization of small molecules in intense laser fields. *J. Phys.* B **26**, 783.

Constant, E., Stapelfeldt, H. & Corkum, P. B. 1996 Observation of enhanced ionization of molecular ions in intense laser fields. *Phys. Rev. Lett.* **76**, 4140.

Corkum, P. B., Ivanov, M. Yu & Wright, J. S. 1997 Subfemtosecond processes in intense laser light. *A. Rev. Phys. Chem.* **48**, 387.

Dietrich, P., Strickland, D. T., Laberge, M. & Corkum, P. B. 1993 Molecular reorientation during dissociative ionization. *Phys. Rev.* A **47**, 2305.

Friedrich, B. & Herschbach, D. 1995 Alignment and trapping of molecules in intense laser fields. *Phys. Rev. Lett.* **74**, 4623.

Harbol, K. L. 1995 A mass spectroscopic investigation of triply charged diatomic molecular species. Ann Arbor, MI: University of Michigan Dissertation Service.

Hurley, M. M., Pacios, L. F., Christiansen, P. A., Ross, R. B. & Ermler, W. C. 1986 *Ab initio* relativistic effective potentials with spin-orbit operators. II. K through Kr. *J. Chem. Phys.* **84**, 6840.

Kanter, E. P., Cooney, P. J., Gemmell, D. S., Groeneveld, K.-O., Pietsch, W. J., Ratkowski, A. J., Vager, Z. & Zabransky, B. J. 1979 Role of excited electronic states in the interactions of fast (MeV) molecular ions with solids and gases. *Phys. Rev.* A **20**, 834.

Mathur, D. 1993 Multiply charged molecules. *Phys. Rep.* **225**, 193.

Nisoli, M., De Silvestri, S., Svelto, O., Szipocs, R., Ferencz, K., Spielmann, Ch., Sartania, S. & Krausz, F. 1997 Compression of high-energy laser pulses below 5 fs. *Opt. Lett.* **22**, 522.

Normand, D., Lompré, L. A. & Cornaggia, C. 1992 Laser-induced molecular alignment probed by a double-pulse experiment. *J. Phys.* B **25**, L497.

Raksi, F., Wilson, K. R., Zhimig Jiang, Ikhlef, A., Cote, C. Y. & Kieffer, J. C., 1996 Ultrafast X-ray absorption probing of a chemical reaction. *J. Chem. Phys.* **104**, 6066.

Sakai, H., Stapelfeldt, H., Constant, E., Ivanov, M. Yu, Matusek, D. R., Wright, J. S. & Corkum, P. B. 1997 *Metastable trication production with femtosecond pulses.* Preprint: National Research Council of Canada, Ottawa.

Schoenlein, R.W. *et al.* 1997 Femtosecond X-ray pulses at 0.4 Å generated by 90° Thomson scattering: a tool for probing the structural dynamics of materials. *Science* **274**, 236.

Seideman, T., Ivanov, M. Yu & Corkum, P. B. 1995 The role of electron localization in intense field molecular ionization. *Phys. Rev. Lett.* **75**, 2819.

Stapelfeldt, H., Constant, E. & Corkum, P. B. 1995 Wave packet structure and dynamics measured by Coulomb explosion. *Phys. Rev. Lett.* **74**, 3780.

Stapelfeldt, H., Sakai, H., Constant, E. & Corkum, P. B. 1997 Formation and measurement of molecular quantum picostructures. *Phys. Rev.* A **55**, R3319.

Stapelfeldt, H., Constant, E., Sakai, H. & Corkum, P. B. 1997 Time resolved femtosecond laser induced Coulomb explosion: a new method to measure structure and dynamics of molecular nuclear wave packets. Preprint, National Research Council of Canada, Ottawa.

Strickland, D. T., Beaudoin, Y., Dietrich, P. & Corkum, P. B. 1992 Optical studies of inertially confined molecular iodine ions. *Phys. Rev. Lett.* **68**, 2755.

Vager, Z., Naaman, R. & Kanter, E. P. 1989 *Science* **244**, 426.

Werner, U., Beckord, K., Becker, J., Folkerts, H. O. & Lutz, H. O. 1995 Ion-impact-induced fragmentation of water molecules. *Nucl. Instr. Meth.* B **98**, 385.

Williamson, J. C., Cao, J., Ihee, H. & Zewail, A. H. 1997 Clocking transient chemical changes by ultrafast electron diffraction. *Nature* **386**, 159.